Subproject A2.7

Growth of Nitride Spin Devices

Principle Investigators: Daniel M. Schaadt

CFN-Financed Scientists: Ralf Schuber (1/2 E13, 24 months), Philipp Ganz (1/2 E13, 13 months)

Further Scientists: Dr. Christoph Sürgers; Prof. Dr. Thomas Schimmel

Institut für Angewandte Physik
Karlsruher Institut für Technologie (KIT)

A2.7 Schaadt

Growth of Nitride Spin Devices

Introduction and Summary

Group III nitride based materials find a variety of applications nowadays and have thus attracted a lot of scientific interest. Their beneficial properties include a band gap that is tuneable through the whole visible spectrum from 0.7 eV (InN) over 3.4 eV (GaN) to 6.2 eV (AlN), depending on the composition of the material. Further, high electron mobility, high thermal, chemical and mechanical stability as well as the non-toxicity of the participating elements are strong arguments for the usage of Nitrides in devices.

1. Non polar GaN films

In order to produce high quality crystals it is necessary to grow nitrides epitaxially onto a suitable substrate. However, this material system, grown along the <0001> direction shows a strong quantum confined Stark effect due to internal electric fields, resulting from the spontaneous and piezoelectric polarization. These fields cause a reduction of the oscillator strength caused by a spatial separation of electrons and holes and a decrease in the energy of the radiative transition.

Epitaxial layers with non-polar surfaces such as the M-plane {1-100} and A-plane {11-20} are attractive due to the absence of built-in electrical fields in growth direction. Moreover, due to the lack of readily available substrates for homoepitaxy, there has been an ongoing search for promising substrates that would lead to high quality GaN crystals. $LiAlO_2$ (LAO) and its chemically similar compound $LiGaO_2$ (LGO) constitute particularly suitable substrates as their lattice mismatch to GaN is very low. Each of these substrates has their own advantages.

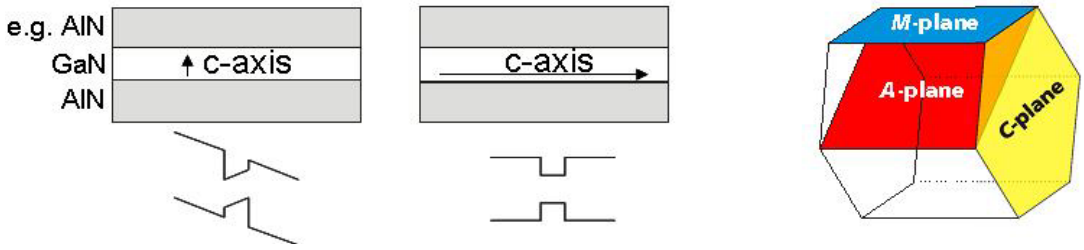

Fig.1: Left: Cartoons indicating the distortion of the band structure schematically, depending on the growth direction of the wurtzite structure. Right: schematic of the wurtzite crystal structure with indication of the *M*-, *A*- and *C*-plane.

The (100) face of γ-$LiAlO_2$, with tetragonal structure, is well lattice matched to both the *M*- and the *C*-plane of GaN and has already been studied in detail for the growth of non polar GaN, e.g. [1, 2]. The substrate can be grown by the Czochralski technique and a lot of effort has already been put into optimizing the polishing of its surface with regards to flatness. However, since both the *M*- and *C*-plane of GaN are lattice matched to the same substrate surface a special growth procedure has to be applied in order to obtain phase purity of the epitaxial layer. Furthermore, because the (100) plane of LAO has two types of surfaces [2] that yield different qualities of GaN an additional factor has to be taken into account when investigations are done.
The orthorhombic β-$LiGaO_2$ is a crystal with lattice constants which match well to the *A*-, *M*- and *C*-plane of GaN. However, each of the GaN planes match to a different plane of LGO, i.e. *M*-plane

GaN matches the (100) LGO, *A*-plane GaN fits onto (010) LGO and the *C*-plane of GaN fits onto (001) LGO. In addition to the possibility to grow GaN in three different crystal directions, including polar and non polar ones, on the same substrate material, this automatically leads to a high phase purity of the epitaxial GaN film. While growth of *C*-plane GaN has already been established on (001) LGO [3], growth of *M*- and *A*-plane GaN on LGO by MBE has first been achieved in this project [4, 5].

Before introduction to the MBE chamber, the LGO substrates were mounted onto Si wafers using a thin In layer to provide a homogeneous thermal coupling. The substrates, placed into molybdenum holders, were outgased for 60 min at 130°C prior to the transfer into the growth chamber. During growth, activated nitrogen N_2 was supplied by an RF plasma cell. Ion deflection plates were used to reduce the ion amount in the nitrogen flux. Growth procedures were monitored *in-situ* using reflective high energy electron diffraction (RHEED). To establish *A*- or *M*-plane GaN growth the substrate temperature was optimized in the range between 650°C and 800°C and the Ga flux was varied from slightly Ga rich to Ga rich conditions. Several pre-growth treatments of the substrate in the growth chamber were studied. These were Ga desorption, nitridation, Ga desorption and nitridation, annealing and no treatment of the substrate.

Successful growth of GaN on LGO was achieved when the substrate was annealed at 800°C for 60 min and temperature ramps were employed carefully. Growth of GaN commenced at slightly Ga rich conditions at a substrate temperature of 700°C. The temperatures given correspond to the thermocouple readings. Irradiation of the sample with the RHEED beam was reduced to a minimum to prevent possible damage to the sample. Shortly after taking the sample out of the growth chamber, the GaN film showed small cracks at the edges. A too high temperature in the area of contact between the substrate and the Mo holder probably was the reason for these features. However, approximately more than 98% of the films remained stable and did not lift-off or show cracks. Characterization of the sample was done ex-situ by x-ray diffraction (XRD) and atomic force microscopy (AFM).

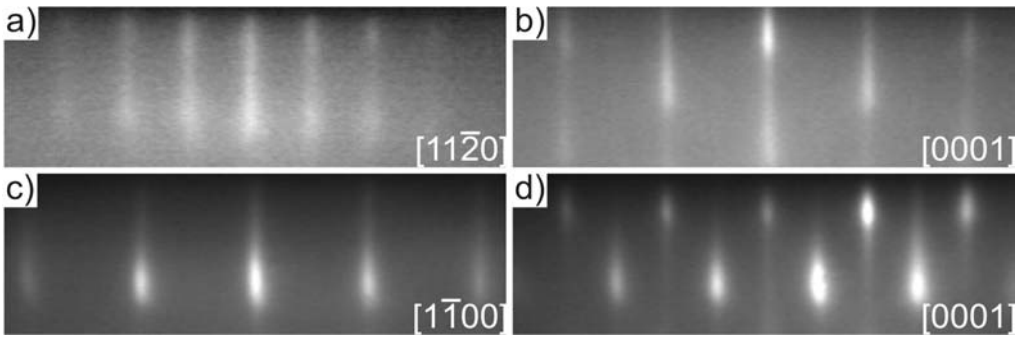

Fig.2: a) and b): RHEED images of the *M*-plane GaN azimuths, separated by 90°. The spacing of the streaks in [11-20] direction gives the c_{GaN} lattice constant whereas the a_{GaN} lattice constant is given by the separation of streaks in [0001] direction. c) and d): RHEED patterns of two perpendicular *A*-plane GaN azimuths. Here the spacing of the streaks in [1-100] direction corresponds to $\sqrt{3}\ a_{GaN}$.

RHEED measurements indicate a smooth film surface by showing streaky diffraction patterns. First evidence of the crystal orientation of the GaN film can be gained by comparing the ratio of the line separation in [0001] direction and the direction perpendicular to it, i.e. the [11-20] and [1-100] direction for *M*-plane and *A*-plane GaN, respectively. Figure 2 a) and b) show the two diffraction

patterns separated by 90° of the *M*-plane GaN sample while the equivalent RHEED patterns of the *A*-plane GaN sample can be seen in Fig. 2 c) and d).

Figure 3 depicts results obtained by x-ray diffraction and AFM measurements on the two samples. Part a) shows two sections of an ω-2θ scan on the *M*-plane GaN film. Part b) shows two regions of the scan of the *A*-plane GaN sample. In both cases the high phase purity of at least 99 % is apparent, i.e. a *C*-plane GaN component in any of the two films is lower than 1 %. From the relative shift of the GaN peaks to the substrate peak, which is assumed to be completely relaxed, the strain state of the films is estimated. The 390 nm thick *M*-plane GaN film is relaxed to roughly 80% compared to the maximal possible transverse deformation caused by the lattice mismatch between the substrate and the GaN film. For the 170 nm thick *A*-plane GaN film a relaxation state of approximately 50% was found.

Although the bulk crystal quality of the substrate, LGO, is very high as determined from x-ray rocking curves (FWHM of (200) LGO and (040) LGO are 23 and 18 arcsec, respectively), the polishing of epi-ready substrates needs improvement. AFM images (not shown here) reveal a large number of surface scratches with root-mean-square (rms) roughness values on the order of 10-20 nm over an area of 10x10 μm^2. These surface scratches originating from the substrate are also seen in AFM images of the surfaces of the GaN epitaxial layers seen in Fig. 3 b) and d) for the *M*-plane and *A*-plane GaN, respectively. The rms value for the *M*-plane GaN surface over 10x10 μm^2 was measured to be as low as 2.9 nm. The *A*-plane GaN surface shows a higher rms value which amounts to about 10 nm in an area of 8x8 μm^2, where an area was considered omitting the most pronounced scratches.

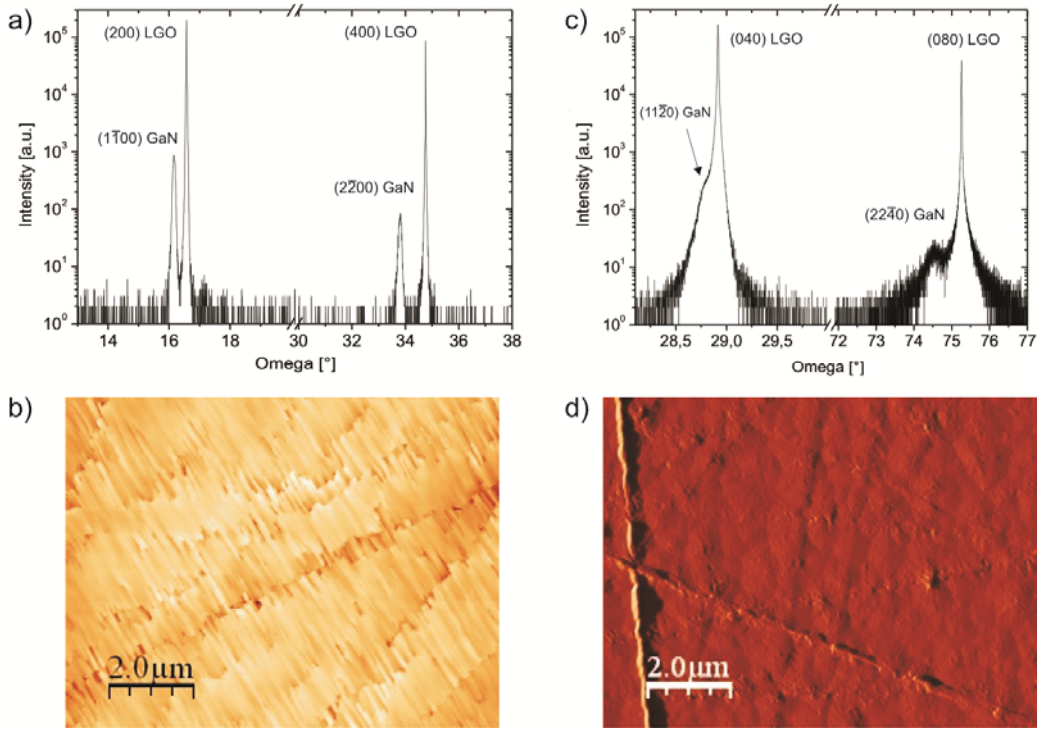

Fig.3: a) and b) show XRD and AFM data of the *M*-plane GaN film grown on (100) LGO. c) and d) depicts XRD and AFM data of the *A*-plane GaN film grown on (010) LGO. The close peak positions of GaN and LGO in the ω-2θ XRD scans indicate the close lattice match of the film with its substrate.

TEM analysis of the GaN films confirms the epitaxial relationship that was already found by RHEED and XRD measurements. Further, threading dislocations and stacking faults are seen to be the major defects present in both films. Fig. 4 a) and b) show bright field images of the *M*-plane and *A*-plane GaN cross sectional TEM samples, respectively, with the plane of the cross section perpendicular to the [0001] direction. The high density of threading dislocations is apparent. In these images stacking faults are not visible, as they lie in the *C*-plane. However, inversion domain boundaries, confining stacking faults, are visible in Fig. 4 b) as straight lines running across the image at an angle of 60°. The plan view TEM sample of the *M*-plane GaN film allows calculation of the density of threading dislocations and stacking faults which lie in the order of 10^{11} cm^{-2} and $2x10^{5}$ cm^{-1}, respectively. Judging from the cross sectional TEM data for the *A*-plane GaN sample a similar value for the density of threading dislocations is expected. However, less stacking faults are present in the *A*-plane GaN film. This can be seen in the cross sectional TEM image cut perpendicular to the [1-100] direction (not shown here). A confirmation of this observation is given by the fact that lines elongated from the diffraction spots in c direction, indicating the presence of stacking faults, are present in the diffraction pattern of the *M*-plane GaN TEM sample (cut perpendicular to the [11-20] direction) but are missing in the *A*-plane GaN sample (cut perpendicular to the [1-100] direction).

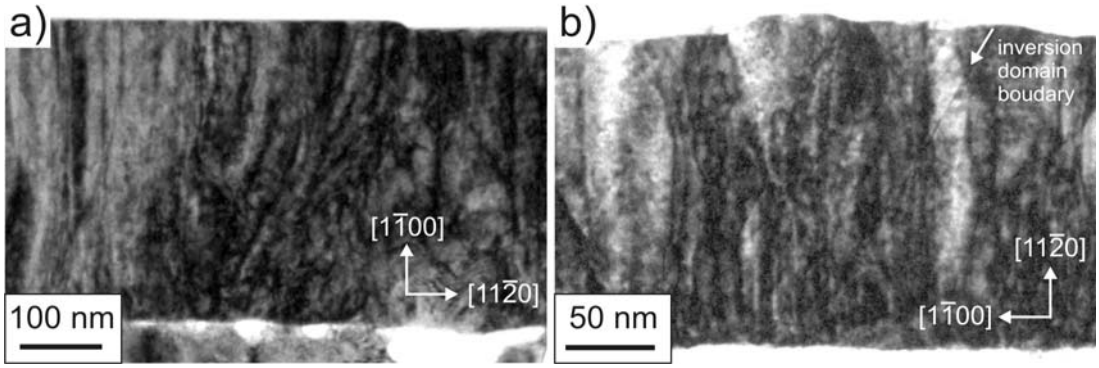

Fig.4: Bright field images taken of the cross sectional TEM samples of the *M*-plane (a) and *A*-plane (b) GaN sample. In both images the observer is looking into the [0001] direction. In each case the substrate is located at the bottom of the picture. The a) sample was cut by FIB, the sample seen in b) was fabricated by mechanical polishing.

The results prove experimentally the expected epitaxial relationship of *M*-plane GaN on (100) LGO and *A*-plane GaN on (010) LGO. From the data collected we find a high phase purity of the grown GaN films. Surface scratches present in the GaN films origin from scratches in the substrate. We expect to obtain smoother surfaces and a higher crystal quality of the GaN films when mechanical polishing of the substrate as well as growth conditions have been optimized. The main defects in the GaN films are threading dislocations and stacking faults.

2. Cu-doped nitrides: Diluted magnetic semiconductors from first principle studies

Dilute magnetic semiconductors (DMS), which are proposed to show ferromagnetism at room-temperature, have raised interest due to their possible applications in spintronic devices. Investigations on the ferromagnetism in DMS usually focus on the doping with transition metals. Semiconducting group-III nitrides are attractive for spintronic applications and devices due to their long and temperature independent spin-lifetime in InN quantum dots [6, 7]. Additionally, these nitrides cover a large bandgap area and have a strong thermal and chemical stability.
The most common GaN-based DMS are Mn-doped GaN and Gd-doped GaN. For both materials, room-temperature ferromagnetism was proposed by theory [8, 9] and was also observed experimentally [10, 11]. However, the origin of the ferromagnetism in these materials is still under debate, because Mn and Gd are intrinsic magnetic elements and, in addition, tends to build clusters in the GaN host [12, 13]. These clusters or precipitates may also cause the observed ferromagnetic behavior. Additionally, these magnetic clusters were also found for Mn- and Gd-doped AlN [14, 15].
To avoid problems with transition metals precipitates that are ferromagnetic, Cu was used as dopand. Cu-doped ZnO was predicted to be ferromagnetic [16] which was confirmed experimentally by Buchholz et al. [17]. Because ZnO and group-III nitrides are comparable semiconductors (both solidify in the wurtzite structure, have nearly the same lattice constants and a direct bandgap of similar energy), Cu might also serve as a dopand to induce ferromagnetic order in group-III nitrides. In theory, Cu-doped GaN has been discussed controversially. Wu et al. [18] proposed a ferromagnetic ground state and a Curie temperature of 350K for a certain Cu arrangement in the nitride host. They also predicted a 100% spin polarization and a magnetization of $2.0\mu_{Bohr}$ per Cu atom. On the contrary, Rosa et al. [19] expect rather weak ferromagnetism in Cu-doped GaN, because Cu atoms tend to be located close to each other in the GaN lattice, leading to a smaller magnetic saturation. The allocation of the Cu atoms near each other should be favorable in energy according to [19]. For Cu-doped AlN, a strong ferromagnetic order was predicted by several groups [20, 21]. However, no calculations were performed for Cu atoms being incorporated in the lattice as interstitials or sitting on nitrogen sites. Also the influence of carriers was not taken into account. Experimentally, room-temperature ferromagnetism was observed in GaN:Cu and AlN:Cu both in bulk material and nanorods. For Cu^{+}-ion implanted GaN, Lee et al. [22] observed a much smaller magnetic moment than predicted by Wu et al. [18]. They found that the value of μ depends sensitively on the annealing conditions suggests that defects, introduced by the ion implantation, play an important role. Nearly the same results were reported for Cu-implanted AlN [23]. Enhanced magnetic saturation, increasing with the Cu dopant level, was observed in calcinated Cu-doped GaN [24] and nanowires [25]. These nanowires exhibit a single-crystalline and defect-free nature which strongly suggests that the ferromagnetic behavior is caused by Cu in the GaN host. Indeed, calculations on Cu-doped GaN nanowires predict an enhanced ferromagnetic stability under conditions, where all dangling bonds are saturated by hydrogen [26]. For further applications, the epitaxial growth of Cu-doped nitrides would be indispensible. Especially, molecular beam epitaxy offers a unique opportunity to grow high quality thin films epitaxially. Initial studies on Cu-doped GaN grown by molecular beam epitaxy were reported by us [27, 28].

The theoretical work on Cu-doped group-III nitrides is very manageable. Additionally, the few existing publications on bulk GaN:Cu material [18, 19] differ in the assumption of the favorable atomic positions which are occupied by the Cu atoms resulting in different magnetic behavior. Therefore, we also performed density functional theory (DFT) calculations using the Wien2k code [29]. The properties were studied on a 2 x 2 x 2 GaN supercell, with two Cu atoms substituting Ga sites. Other defects such as vacancies or interstitial atoms were not considered. For the calculation of the exchange-correlation potential, the general gradient approximation (GGA) within the PBE

scheme [21] was used. A 7 x 7 x 4 k mesh was used to scan the irreducible Brillouin zone. The convergence criterion was set to 1.4 meV for the total energy. All calculations were obtained for wurtzite GaN with the lattice constants a = 0.3189 nm and c = 0.5189 nm. After structural optimization, a marginal change in the lattice constants was observed.

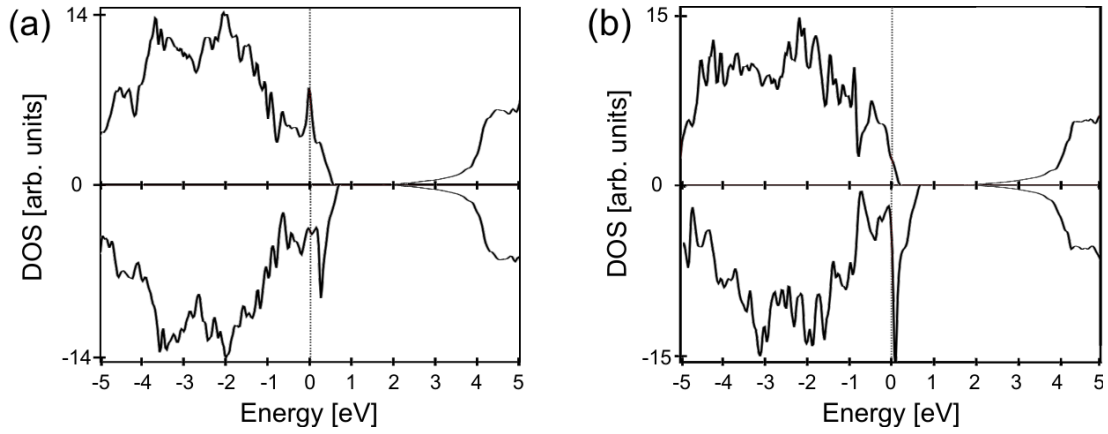

Fig. 5: Spin-up (top) and spin-down (bottom) for "far" (a) and "close" (b) Cu arrangement.

Our calculations are made for two Cu atoms in the supercell corresponding to a high Cu concentration of 12.5 at.%. The Cu atoms were put on Ga sites. Figure 5 shows the electronic density of states (DOS) for the spin-up and spin-down channels for the "far" configuration (Fig. 5a), corresponding to a Cu-Cu distance of 0.5169 nm, and for the "close" configuration (Fig. 5b), corresponding to a Cu-Cu distance of 0.2986 nm, respectively. For both, a high spin-polarization of about 90% is observed. For the "far" configuration, we obtain a semiconductor-like DOS for the spin-up channel and a metallic behavior for the spin-down channel. The energy difference between these two spin states is about 600 meV. However, for the "close" configuration, the energy difference is about 300 meV, much lower than for the "far" configuration. There is also a little change in the band arrangement. For the "close" configuration, the spin-up states are more in the valence band and the spin-down states are slightly above zero energy, which corresponds to the valence band edge.

Cu-doped group-III nitrides were grown by plasma-assisted molecular beam epitaxy on *C*-plane sapphire substrates. The substrates were glued onto silicon wafers with indium for good heat transfer. Nitridation of the sapphire surface, which is the crucial point to obtain high quality nitride films, was performed at a temperature of 200 °C (thermocouple reading) in an activated nitrogen flux with a pressure of 3.2×10^{-5} Pa. After nitridation, a 25-nm thick AlN buffer layer was deposited under Al-rich conditions. Subsequently, Cu-doped GaN or AlN was grown at a substrate temperature of 790°C. A slow growth rate of 70 nm per hour was used to obtain good crystalline film quality with typical thickness of 140 nm.

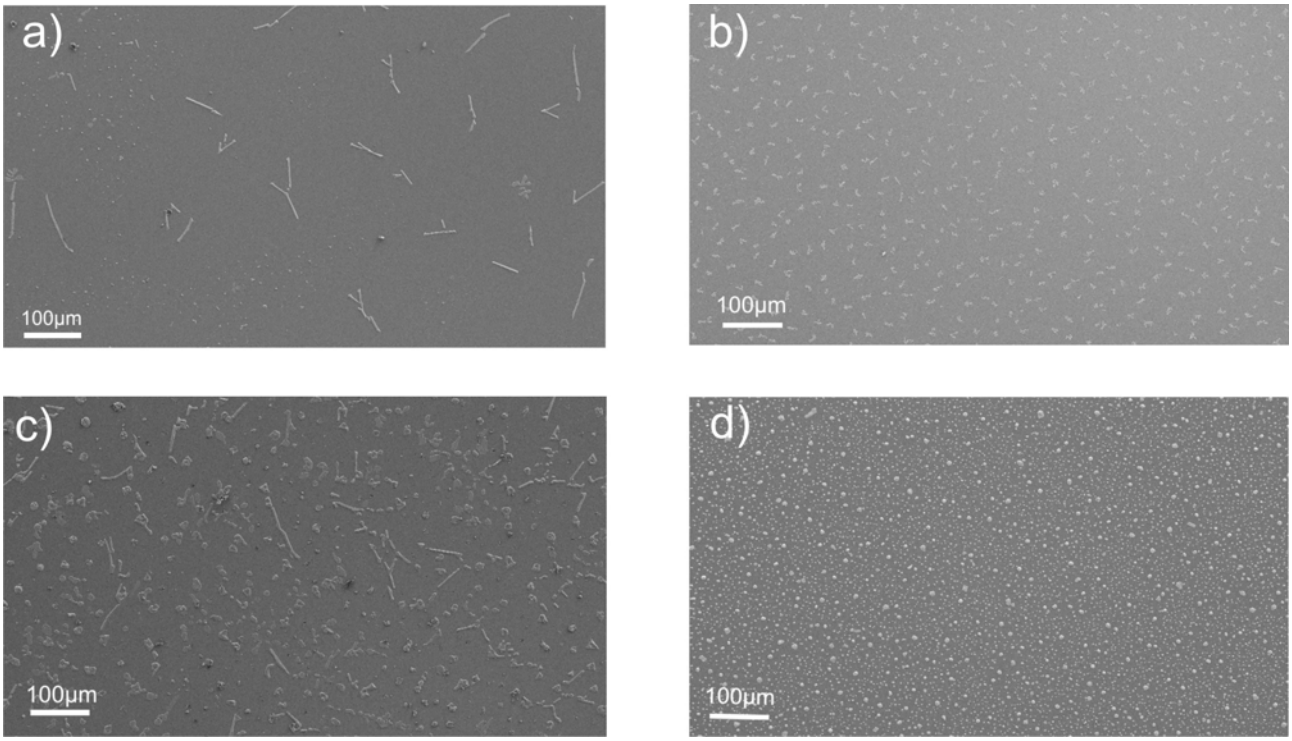

Fig. 6: SEM images of the surface of GaN:Cu for different Cu-to-Ga beam equivalent pressure (BEP) ratios from 1.2% (a) to 2.0% (b) up to 4.8% (c) and an AlN:Cu (d), obtained by the Nanostructure Service Laboratory.

All our Cu-doped samples show typically the formation of islands on top of the surface for both Cu-doped GaN (Fig. 6a-c) and AlN (Fig. 6d). However, the surface next to the islands is very smooth, which is indicated by thin and streaky RHEED (reflection of high energy electron diffraction) patterns as well as by atomic force microscopy (AFM). The average roughness of the surface without the islands is calculated to be 1.6 nm. With increasing the amount of Cu, the surface roughness stays at the same value. However, the size and the amount of the islands increase strongly.
To determine the composition of these islands, energy-dispersive X-ray spectroscopy (EDX) was performed. Fig. 7 shows EDX spectra acquired with excitation energy up to 10 keV.

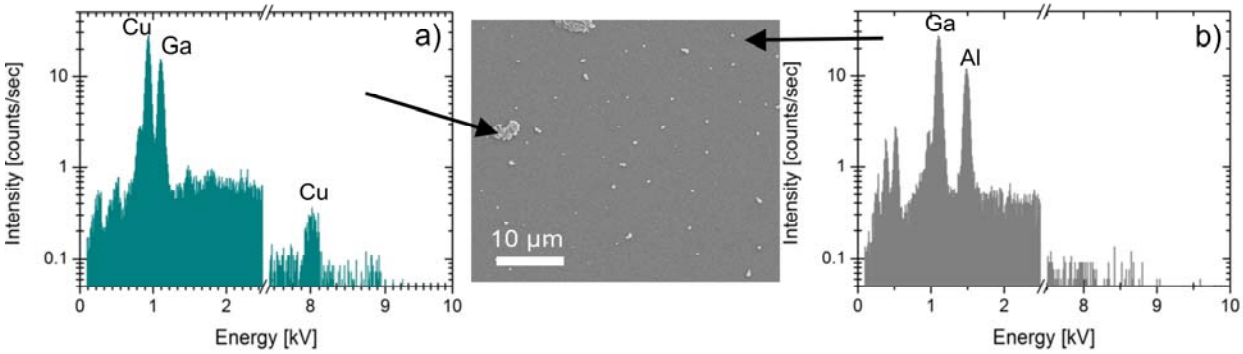

Fig. 7: EDX spectra of (a) an island on the surface and (b) the epitaxial film.

Fig. 7a) shows the measurement for the island. Two main peaks appear at 0.95 keV and 1.11 keV. The first peak is due to the Cu L-edge, the second due to the Ga L-edge. Additionally, a small peak

can be seen around 8.04 keV, which is due to the Cu K-edge. Both measurements on islands show a high Cu concentration of about 60 at.%. While a large Cu concentration is measured in these precipitates, little or no Cu could be detected in the epitaxial layer within the 1-2 at.% detection limit of the used EDX setup, as shown in Fig. 7b). The Cu peak at 0.95 keV is hardly visible and the peak at 8.04 keV disappears completely, even for higher excitation energy of 15 keV. An additional peak at 1.5 keV can be ascribed to aluminum. The Al contribution to the spectra results from the AlN buffer layer and from the sapphire substrate. Only a few binary alloys of Cu and Ga exist, namely $CuGa_2$, Cu_3Ga and Cu_9Ga_4 [30]. Our EDX results, shown in figure 7 indicated a Cu composition of about 60 at.%. Therefore, the islands must consist of Cu_9Ga_4.

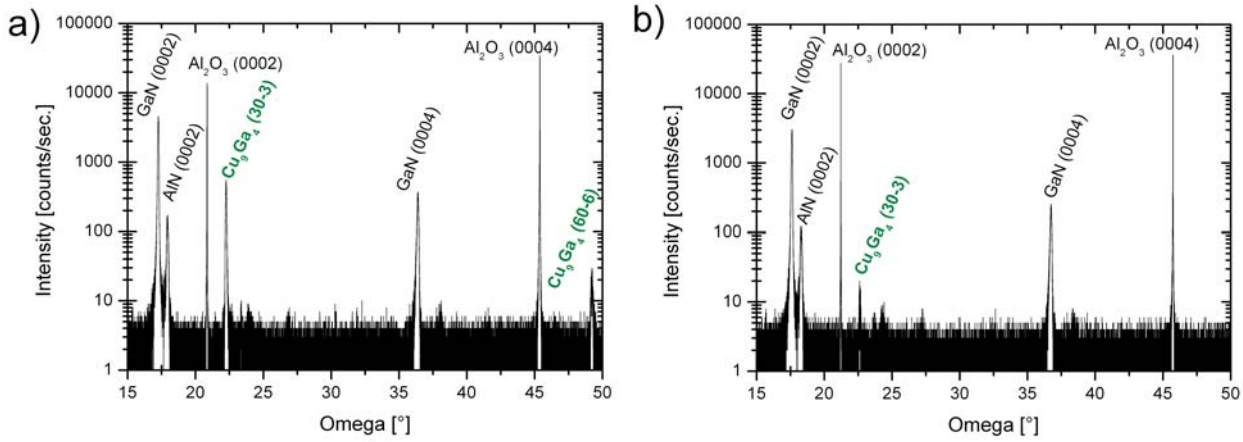

Fig. 8: a) X-ray diffraction spectra for as grown Cu-doped GaN. A narrow peak for GaN is observed as well as a signal from the Cu-Ga islands. (b) shows the XRD spectra after etching with HNO3 for minutes. The peak of the Cu-Ga islands at 22.4° was highly reduced; the second peak around 49.2° disappeared completely.

A method to indicate secondary phases and to get information about the crystalline quality of a sample is X-ray diffraction (XRD). Figure 8a) shows the results for the as grown Cu-doped GaN with 1.2% nominal doping. For GaN, a very narrow peak is observed. The full width half maximum of this peak measured from the rocking curve is about 280 arcsec. The observed AlN (0002) peak is due to the AlN buffer layer. Additionally, two peak around 22.4° and 49.2°were detected. These two peaks were ascribed to the Cu-Ga islands on the surface. Knowing the composition of these islands by EDX, we found that these additional peaks, which could not be detected in the XRD spectra for pure GaN, are Bragg peaks for the (30-3) and (60-6) crystal orientation of Cu_9Ga_4. For further applications of these diluted magnetic semiconductors, we tried to get rid of these islands. Wet chemical etching is very convenient for etching additional compounds on group-III nitrides surfaces because nitrides are very stable. Etching with HNO_3 for 5 minutes was performed on the Cu-doped nitrides. The results for Cu-doped GaN are detected by XRD and shown in Fig. 8b). Compared to figure 8a), the right Cu-Ga peak (49.2°) disappears completely after etching. Over 90% of the counts for the major peak of the Cu-Ga compounds at 22.4° are lost. However, etching, even for longer times, could not remove the Cu-Ga islands completely.
For Cu-doped AlN samples, the results for the surface morphology are very similar to these of Cu-doped GaN. Instead of the formation of Cu_9Ga_4 on the surface, Cu_9Al_4 is growing on the surface.

As the Cu-metal compounds have no influence on the magnetic properties because of their metallic character, the SQUID measurements are performed on non-etched samples. The ferromagnetic behavior of Cu-doped group-III nitrides was explored by superconducting quantum-interference device (SQUID) magnetometry between 10 K and 400 K with the magnetic field applied parallel to the film plane. A ferromagnetic signal with small coercivity is observed even at room-temperature

(Fig. 9a) for the 1.2 % GaN:Cu sample. For comparison, the diamagnetic behavior of pure GaN is also shown. Similar hysteresis loops with small coercivity have been reported earlier for various DMS [24-26]. After subtraction of the diamagnetic contribution to the magnetic properties from the GaN and the sapphire substrate, the curves in figure 9b) are obtained. Cu-doped GaN saturates when a magnetic field of about 50 mT is applied. The saturation magnetization of 0.8 emu per cm³ does not change with the temperature. An important issue for possible spintronic applications is the Curie temperature T_C. We found that our non-etched MBE-grown Cu-doped GaN shows ferromagnetic behavior even at 400 K (Fig. 9c). To exclude the Cu-Ga islands on the surface cause the ferromagnetic behavior, we intentionally deposited Cu-Ga alloys on top of pure GaN at a low temperature to avoid Cu incorporation in the GaN lattice. This sample shows diamagnetic behavior. Therefore, the observed ferromagnetic behavior must be caused by Cu incorporation in the GaN lattice. For higher doping levels like 2.0%, but also lower doping levels like 0.5%, only diamagnetism was observed. This assumes that there is a small range for having ferromagnetic order in Cu-doped GaN. In contrast, Cu-doped AlN shows only diamagnetic behavior (Fig. 9d). No ferromagnetic behavior is found for Cu to Al BEP ratios from 1.0 to 4.0%.

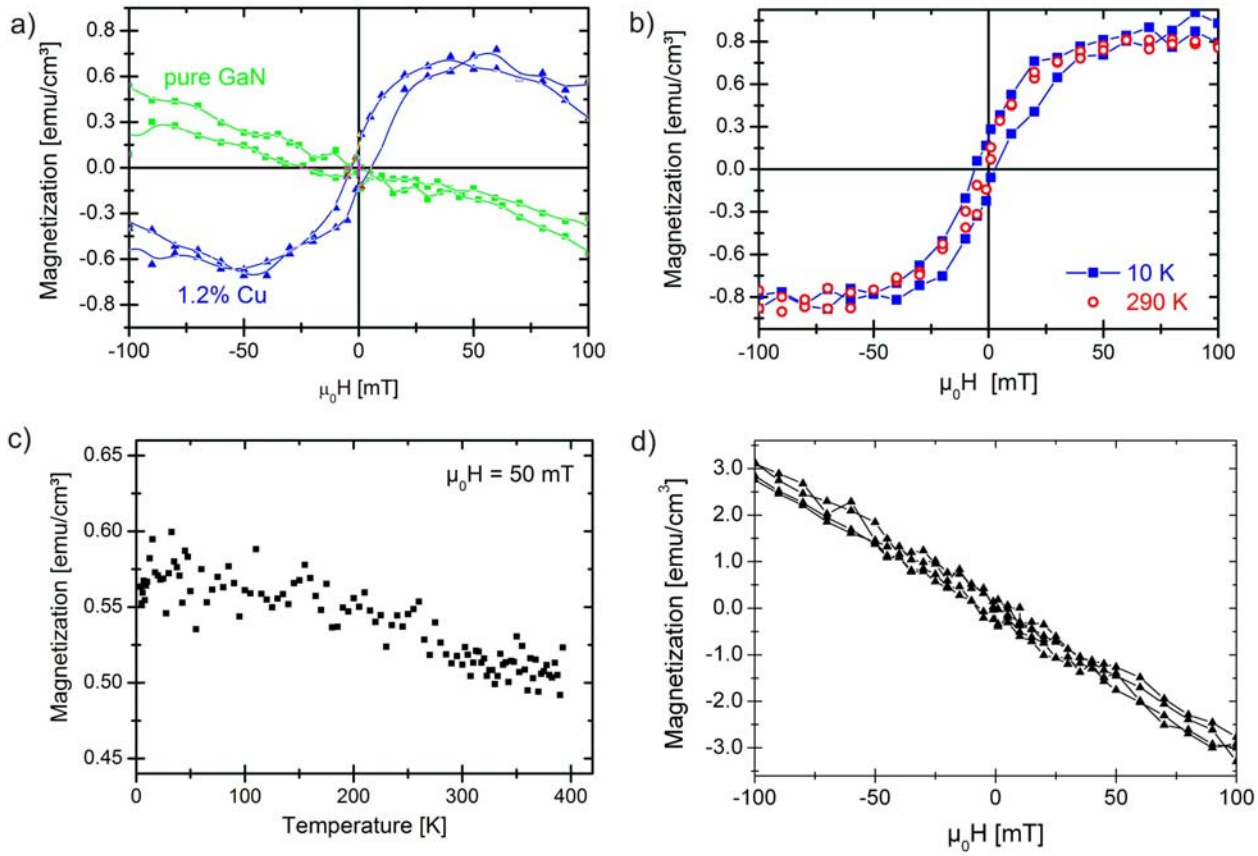

Fig. 9: (a) Magnetization M versus magnetic field H of pure GaN and of Cu-doped GaN for the 1.2% Cu to Ga BEP ratio sample at T=290K as measured. (b) Magnetization of the 1.2% Cu-doped GaN after subtraction of the diamagnetic contribution of the substrate and pure GaN. (c) Ferromagnetic behavior of Cu-doped GaN even at a temperature of 400~K. For samples with higher nominal Cu concentration, only diamagnetic behavior was found (d).

As the origin of ferromagnetic behavior in Cu-doped GaN is still unclear, a detailed understanding of the incorporation of Cu in the GaN host is desirable. Cu could be incorporated in the GaN lattice

on Ga sites inducing ferromagnetic behavior by Zener double exchange or p-d hybridization mechanism [18]. On the other hand, the incorporation of Cu may cause magnetic lattice defects, such as point defects, interstitials, voids, dangling bonds etc., which may also be an origin of the ferromagnetic behavior [31].

A way of probing the local electronic structure of Cu-doped GaN is given by element specific x-ray absorption spectroscopy (XAS). Especially x-ray linear dichroism (XLD) is a suitable technique to explore the local structure and symmetry of a material by probing the anisotropy of the electronic structure [32]. We therefore measured the XLD as well as the x-ray absorption near edge structure (XANES) at the Cu and Ga K-edges of GaN:Cu wurtzite DMS samples at the ID12 beamline of the European Synchrotron Radiation Facility (ESRF). In this way we investigated GaN:Cu samples with nominal Cu concentrations between 0% and 2.3%. To remove the Cu_9Ga_4 compounds from the surfaces the samples were etched with HNO_3 for 5 min. XAS spectra were measured for etched and unetched samples.
For clarification of the experimental results, i.e. to clarify the role of the surface compounds and to evaluate the Cu site position in the GaN host, i.e. Cu on Ga sites, N sites or interstitial sites, we performed simulations of the GaN:Cu and the Cu_9Ga_4 crystals for the Cu and Ga K-edges at different doping levels using the FDMNES code [33]. A comparison with the experimental results shows that the Cu atoms predominantly occupy Ga and interstitial sites.

References

[1] P. Waltereit et al., Nature **406**, 865 (2000)
[2] Y.J. Sun et al., J. Appl. Phys. **92**, 5714 (2002)
[3] M.A.L. Johnson et al., J. Cryst. Growth **175/176**, 72 (1997)
[4] R. Schuber, M.M.C. Chou and D.M. Schaadt, *Growth of M-plane GaN on (100) $LiGaO_2$ by plasma-assisted molecular beam epitaxy*, Thin Solid Films **518**, 6773 (2010)
[5] R. Schuber, M.M.C. Chou, P. Vincze, Th. Schimmel and D.M. Schaadt, *Growth of A-plane GaN on (010) $LiGaO_2$ by plasma-assisted MBE*, J. Cryst. Growth **312**, 1665 (2010)
[6] S. Nagahara, M. Arita, Y. Arakawa, *Appl. Phys. Lett*. **86**, 242103 (2005)
[7] S. Nagahara, M. Arita, Y. Arakawa, *Appl. Phys. Lett.* **88**, 083101 (2006)
[8] K. Sato, H. Katayama-Yoshida, *Jpn. J. Appl. Phys.* **2**, Part 2, L485 (2001)
[9] G. M. Dalpian, S. H. Wei, *Phys. Rev. B* **72**, 115201 (2005)
[10] G. T. Thaler et al., *Appl. Phys. Lett.* **80**, 3964 (2002)
[11] S. Dhar, et al., *Phys. Rev. B* **72**, 245203 (2005)
[12] J. M. Baik, H. W. Jong, J. K. Kim, J. L. Lee, *Appl. Phys. Lett.* **82**, 583 (2003)
[13] S. Dhar, et al., *Appl. Phys. Lett.* **82**, 2077 (2003)
[14] Y.Y. Song et al., J. Magn. Magn. Mater. **290-291**, 1375 (2005)
[15] S.W. Choi et al., *Phys. Status Solidi C* **3 (6)**, 2250 (2006)
[16] X. Feng, *J. Phys.: Condens. Matter* **16**, 4251 (2004)
[17] D. B. Buchholz et al., *Appl. Phys. Lett.* **87**, 082504 (2005)
[18] R. Q. Wu et al., *Appl. Phys. Lett.* **89**, 062505 (2006)
[19] A. L. Rosa, R. Ahuja, *Appl. Phys. Lett.* **91**, 232109 (2007)
[20] Q.Y Wuet al., *J. Phys.: Condens. Matter* **19**, 056209 (2007)
[21] W. Jia et al., *Appl. Phys. Lett.* **101**, 113918 (2007)
[22] J. H. Lee et al., *Appl. Phys. Lett.* **90**, 032504 (2007)
[23] F. Y. Ran et al., *Appl. Phys. Lett.* **95**, 112111 (2009)
[24] B. Seipelet al., *J. Mater. Res.* **22** (5), 1396 (2007)
[25] H. K. Seonget al., *Nano Lett.* **7** (11), 3366 (2007)
[26] H. J. Xiang and S. H. Wei, *Nano Lett.* **8** (7), 1825 (2008)

A2.7 Schaadt

[27] P. R. Ganz, C. Sürgers, G. Fischer, D M Schaadt, *Cu-doped GaN grown by molecular beam epitaxy, J. Phys.: Conf. Series* **200**, 062006 (2010)

[28] P. R. Ganz, G. Fischer, C. Sürgers and D.M. Schaadt, *Cu-doped nitrides: Promising candidates for a nitride based spin-aligner*, *J. Cryst. Growth*, in press: doi:10.1016/j.jcrysgro.2010.10.

[29] P. Blaha, K. Schwarz and P. Sorati, Comp. Phys. Communications **59**, 339 (1990)

[30] Y. Zhang et al., J. Alloys Compounds **438**, 158 (2007)

[31] J. Hong, *J. Appl. Phys.* **103**, 063907 (2008)

[32] Wilhelm et al., AIP Conf. Proc., 879, 1675 (2007).

[33] Y. Joly, Phys. Rev. B, 63, 125120 (2001).